Applied Surface Science 374 (2016) 229–234

Contents lists available at ScienceDirect

Applied Surface Science

journal homepage: www.elsevier.com/locate/apsusc

Fs-laser processing of medical grade polydimethylsiloxane (PDMS)

P.A. Atanasov[a,*], N.E. Stankova[a], N.N. Nedyalkov[a], N. Fukata[b], D. Hirsch[c], B. Rauschenbach[c], S. Amoruso[d], X. Wang[d], K.N. Kolev[e], E.I. Valova[e], J.S. Georgieva[e], St.A. Armyanov[e]

[a] Institute of Electronics, Bulgarian Academy of Sciences, 72 Tsaridradsko shose Blvd., Sofia 1784, Bulgaria
[b] International Centre for Materials for NanoArchitectonics (MANA), National Institute for Materials Science (NIMS), 1-1Namiki, Tsukuba 305-0044, Japan
[c] Leibniz Institute of Surface Modification (IOM), Permoserstrasse 15, D-04318 Leipzig, Germany
[d] Dipartimento di Fisica Università degli Studi di Napoli Federico II and CNR-SPIN, Complesso Universitario di Monte S.Angelo, Via Cintia, I-80126 Napoli, Italy
[e] Rostislaw Kaischew Institute of Physical Chemistry, Bulgarian Academy of Sciences, Acad. G. Bonchev Str., Block 11, Sofia 1113, Bulgaria

ARTICLE INFO

Article history:
Received 26 May 2015
Received in revised form 15 October 2015
Accepted 17 November 2015
Available online 27 November 2015

Keywords:
PDMS-elastomer
IR
VIS and UV fs-laser processing
μ-Raman spectrometry
AFM and SEM analyses
Metallization

ABSTRACT

Medical grade polydimethylsiloxane (PDMS) elastomer is a biomaterial widely used in medicine and high-tech devices, e.g. MEMS and NEMS. In this work, we report an experimental investigation on femtosecond laser processing of PDMS-elastomer with near infrared (NIR), visible (VIS) and ultraviolet (UV) pulses. High definition trenches are produced by varying processing parameters as laser wavelength, pulse duration, fluence, scanning speed and overlap of the subsequent pulses. The sample surface morphology and chemical composition are investigated by Laser Microscopy, SEM and Raman spectroscopy, addressing the effects of the various processing parameters through comparison with the native materials characteristics. For all the laser pulse wavelengths used, the produced tracks are successfully metalized with Ni via electro-less plating method. We observe a negligible influence of the time interval elapsed between laser treatment and metallization process. Our experimental findings suggest promising perspectives of femtosecond laser pulses in micro- and nano-fabrication of hi-tech PDMS devices.

1. Introduction

Polydimethilsiloxane (PDMS) belongs to silicones, a family of polymeric materials whose backbone is composed by an alternate succession of Si and O atoms joined together via strong, covalent inter-atomic bonds. The Si atoms are coupled to two adjacent O atoms and two organic radicals, i.e. C—H or C—R, R being an organic group. The various elements of the silicones group differ only for the organic radicals, e.g. methyl (—CH), vinyl (—HC=CH), hydrocarbons and other organic functional groups. Silicone rubber also falls in this class, but usually includes some additives as fillers, plasticizers, and cross-linkers. Silicones are neutral and chemically stable, have high molecular weight (greater than 5×10^5 g/mol), exhibit very low electrical conductivity and are transparent to visible and near infra-red light. They usually absorb ultraviolet (UV) light at wavelengths below 280 nm (i.e. photon energy above 4.4 eV). Due to their chemical inertness, silicones are perfect biocompatible materials and are widely used as medical implants, e.g. shunts and pacemakers [1], long term neural implants [2,3], micro-channeled tracks as electrodes for neural interfaces for monitoring and/or stimulation of neural activity [4,5]. Chemical species coupling to silicone can only occur through an irreversible breaking of its interatomic bonds [6,7], and mechanical or thermal processes cannot be used because silicone does not melt, sublimate or evaporate but condenses and transforms in a glassy and extremely fragile material at temperature larger than 230 °C.

PDMS is a flexible elastomer and an excellent material for the micro-fabrication of MEMS devices [8]. PDMS surface can be chemically modified in order to obtain the interfacial properties of interest [9]. PDMS can be covalently functionalized by exposing its surface to a reactive oxygen plasma which transforms Si—CH_3 groups into Si—OH groups. These silanol surfaces are easily transformed with alkoxysilanes to yield much different chemistry [10,11].

Laser irradiation offers another advanced and precise method for selective surface processing and functionalization of silicone

* Corresponding author.
E-mail address: paatanas@ie.bas.bg (P.A. Atanasov).

http://dx.doi.org/10.1016/j.apsusc.2015.11.175
0169-4332/

elastomer [7,12–15]. In earlier investigations, we have addressed PDMS-elastomer processing with UV and visible (vis) laser pulses with fs and ns duration [16,17]. μ-Raman spectrometry demonstrated a well-defined dependence of the processed samples on laser pulse fluence, duration, wavelength and number of pulses and successful metallization of the laser processed traces with Pt or Ni was accomplished via electro-less plating. Here we further extend our study of fs laser processing of PDMS-elastomer by using near-infrared (NIR, 1055 nm), VIS (527 nm) and UV (263 nm) fs-laser pulses. High definition trenches are produced for all three different wavelengths. Laser Microscopy (LM) and μ-Raman spectroscopy are exploited to address the role of laser fluence and scanning speed on the morphology and chemical composition of the processed PDMS surface. The produced trenches are, successively, metalized with Ni via electro-less plating, and investigated by scanning electron microscopy (SEM). Interestingly, the metallization is found to be not sensitive to the time interval elapsed after the laser treatment.

2. Experimental

The laser source is a chirped-pulse-amplification Nd:glass system providing pulses at the fundamental wavelength of ≈1055 nm with duration of ≈0.9 ps, at a repetition rate of 33 Hz. Second harmonic-pulse compression of the fundamental output allows generating pulses with a duration of ≈300 fs at 527 nm. UV pulses at 263 nm are obtained through second harmonic generation of the visible output.

The laser beam is focused on the sample surface by using a lens with a focal length of 40 mm. The beam hits the sample surface at normal incidence. The beam diameter on the sample surface is 98 μm for UV, 107 μm for VIS and 108 μm for NIR wavelengths, respectively. In all experiments, the energy per pulse is varied between 60 and 320 μJ by using neutral density filters, and the corresponding laser fluence varies in the range 0.75–4.2 J/cm^2.

The samples are PDMS sheets (Statice Sante MED 4860) with a thickness of 0.25 mm deposited on glass substrates. This specific silicone is PDMS filled with different quantity of silica foam (nanodispersed SiO_2). The PDMS samples are mounted on a computer controlled translation stage. Experiments were carried out at two scanning speeds of 38 μm/s and 95 μm/s, which correspond to 83 and 33 overlapping pulses, respectively. The details of the number of the processed samples and the corresponding values of the experimental parameters are summarized in Table 1.

Samples characterization is carried out by means of a VK-9700K Color 3D Laser Microscope (KEYENCE, Japan) and a RMS-310 μ-Raman spectrometer (Photon Design, Japan). The μ-Raman spectrometer uses an excitation wavelength of 532 nm and has resolution of 0.2 cm^{-1} and image dimension <1 μm^2. The samples are electro-less metalized with Ni several weeks after the laser treatment by following the procedure described in Ref. [11], and analyzed by using a scanning electron microscope SEM (Zeiss Ultra 55, Gemini).

Table 1
Experimental conditions used to process PDMS samples and values of some experimental parameters.

λ = 263 nm UV light	Fluence 0.75–2.20 J/cm^2	7 samples	Two speeds of the x-table: 95 μm/s (33 overlapping pulses) and 38 μm/s (83 subsequent pulses)
λ = 527 nm VIS light	Fluence 0.70–3.20 J/cm^2	7 samples	Two speeds of the x-table: 95 μm/s (33 overlapping pulses) and 38 μm/s (83 subsequent pulses)
λ = 1055 nm NIR light	Fluence 0.80–4.00 J/cm^2	8 samples	Two speeds of the x-table: 95 μm/s (33 overlapping pulses) and 38 μm/s (83 subsequent pulses)

3. Results and discussions

We observe the creation of well-defined, good quality trenches after UV, VIS and NIR fs-laser treatment. As an example, Fig. 1 reports spatial profiles of some of the produced trenches. Depth and width of the trenches depend on wavelength, laser pulse fluence and scanning speed. Fig. 2(a) and (b) shows the variation of trench depth as a function of laser pulse fluence for the three laser pulses investigated, at the two scanning speeds of 95 μm/s (panel (a), 33 overlapping pulses) and 38 μm/s (panel (b), 83 overlapping pulses). In all cases, we observe an almost linear dependence of the trench depth on laser fluence. Moreover, the increase of the scanning speed results in a corresponding decrease of the depth due to the reduced number of overlapping laser pulses. At a fixed fluence value, we generally observe a larger depth for UV with respect to VIS pulses with the same pulse duration, in agreement with earlier reports [16]. This can be rationalized by the higher absorption of the material for UV with respect to VIS light. However, at similar fluence level, NIR fs pulses generally leads to a trench deeper than that corresponding to VIS and UV. The different laser ablation efficiency can depend on the very low absorption of PDMS in the NIR that allows coupling photon energy at longer depths in the sample with respect to lower wavelengths. The different laser pulse duration as well as possible incubation effects related to the laser photon wavelength can also play a role. [18]

The chemical changes induced by laser irradiation are analyzed exactly into the bottom of the trenches by μ-Raman spectrometer, and compared to that of the native material (see Fig. 3(d)). Fig. 3 reports the Raman spectra. No significant changes to the general features of the Raman spectrum are observed when processing the PDMS with UV light (see Fig. 3(a)). However, the intensity of the peaks corresponding to the Si—O—Si, Si—C and methyl stretching bonds gradually decreases with the laser fluence and number of the pulses, which is consistent with Refs. [16,17]. Instead, in the case of VIS or NIR laser processing a sharp peak between 512 cm^{-1} and 518 cm^{-1} ascribed to single crystalline silicon (c-Si) [19] appears in the Raman spectra (see Fig. 3(b) and (c)). The intensity of such a peak increases with the number of pulses and laser fluence with respect to the decrease of the intensity of the peaks of the native material. This could be explained by breaking of the corresponding chemical bonds and chemical transformation of the material caused by laser processing. Additionally, when processing with NIR light at higher fluence and number of overlapping pulses, a strong carbonization appears (see the inset in Fig. 3(c)) accompanied by adjacent cracks of the material in the surrounding areas. The broad peaks between 1340 cm^{-1} and 1360 cm^{-1} and in the wavenumber range 1570–1600 cm^{-1} are related to the D (breathing mode) and G (stretching mode) bands, respectively, of sp^2 bonds in amorphous carbon, namely revealing the formation of highly disordered graphite structures, whereas the Raman peak about 1332 cm^{-1} could due to the presence of fraction of sp^3 carbon bonds [17,20,21].

This decomposition of the organic material by breaking its chemical bonds and transformation and production of inorganic species (Si and C) as result of laser treatment is a base of next technological operation – metallization of the trenches. The electro-less metallization with Ni is applied to samples processed with the three different laser pulses. Table 2 summarizes the results of the

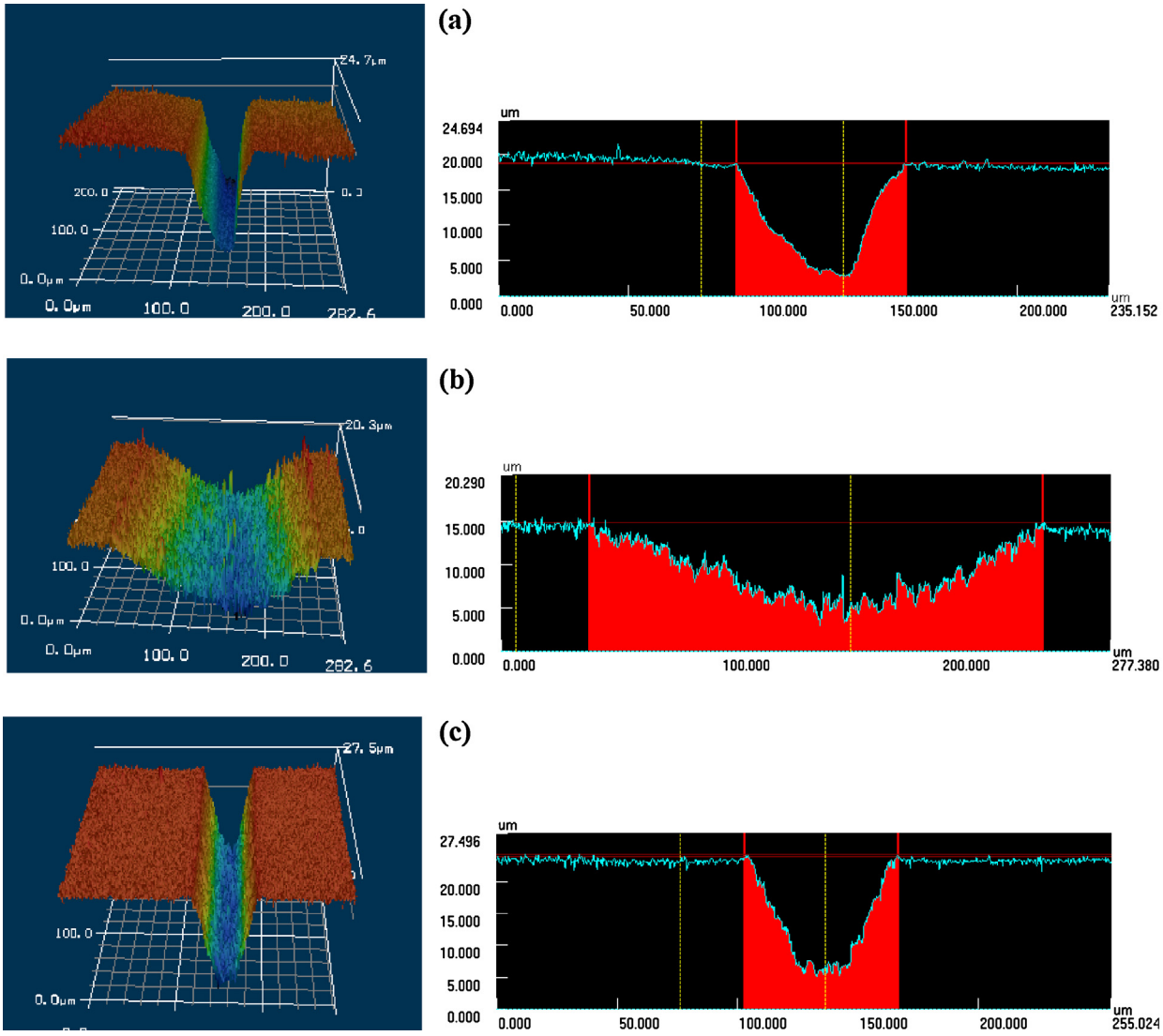

Fig. 1. Pictures of the trenches produced by UV, VIS and NIR fs laser pulses, respectively. (a) UV processing: laser energy = 79 μJ, speed = 38 μm/s, depth of trench – 15.5 μm and width – 62.2 μm; (b) VIS processing: laser energy = 142 μJ, speed = 38 μm/s, depth of trench – 9.3 μm and width – 206.1 μm; (c) NIR processing: laser energy = 307 μJ, speed = 95 μm/s, depth of trench – 16.8 μm and width – 63.5 μm.

electro-less metallization of the fs-laser processed PDMS samples with Ni. Table 2 indicates that good quality and uniform metallization is achieved in the following cases: UV light – for all fluences and larger number of overlapping pulses (83); VIS light – for all fluences and larger number of overlapping pulses (83); NIR light – practically for both number of overlapping pulses and all fluences.

Fig. 4(a–c) reports examples of typical high resolution SEM pictures of metalized trenches after UV, VIS and NIR fs-laser treatment,

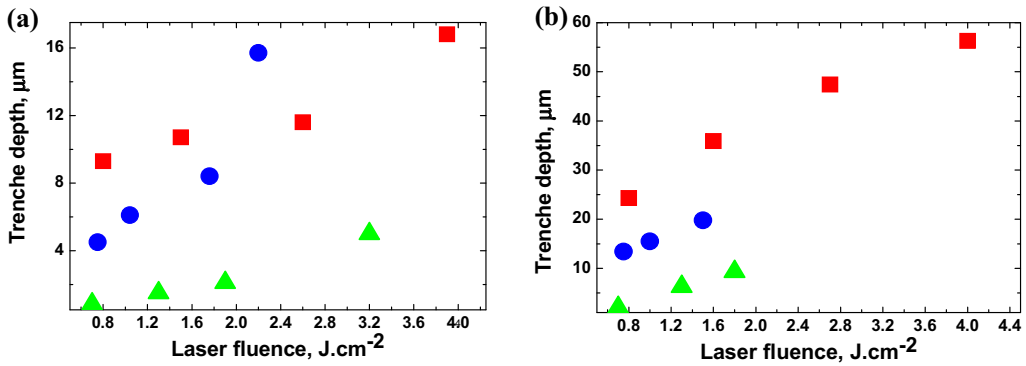

Fig. 2. Dependence of the trench depth on the laser fluence for UV (dots), VIS (triangles) and NIR (quadrates) laser light, respectively. (a) 33 overlapping pulses – 95 μm/s; (b) 83 overlapping pulses – 38 μm/s.

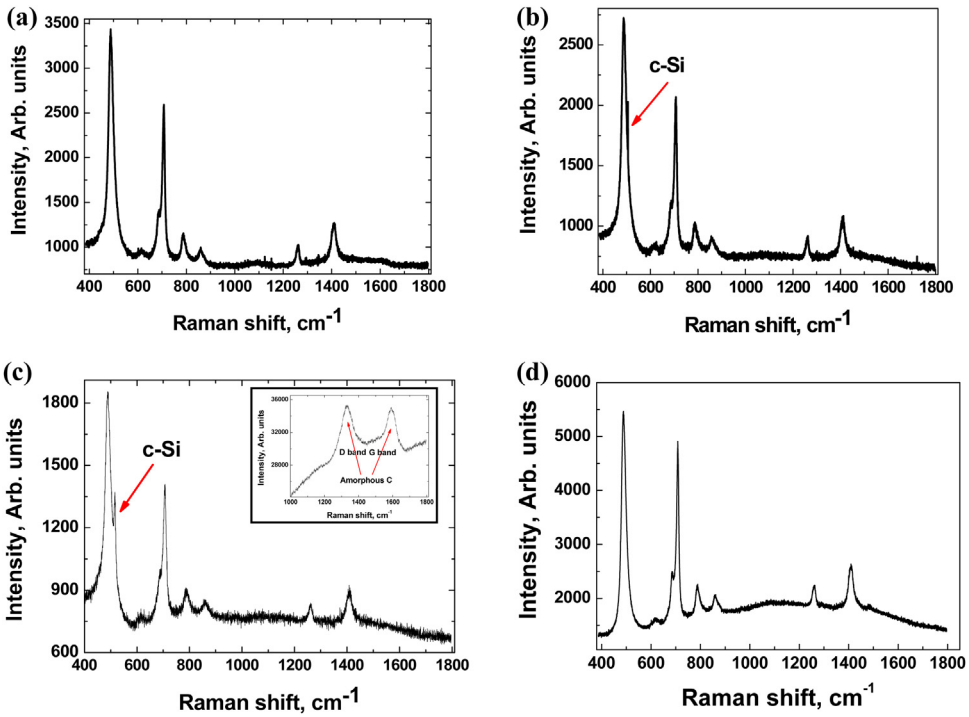

Fig. 3. μ-Raman spectra taken from the bottom of the tracks produced by: (a) UV; (b) VIS; (c) NIR laser light. (d) Reports the μ-Raman spectrum of the non processed PDMS sample. The spectra correspond to the cases given in Fig. 1(–c). The inset in (c) illustrates the appearance of two amorphous carbon G and D bands.

respectively. One can observe an intriguing morphology of the metalized surface, which presents in the form of an assembly of complex nanostructures with the Ni crystallites showing "teeth" or "flower" like shapes. Flower-like structures predominates in the case of UV and VIS laser pulses, while NIR leads to a larger fraction of bigger cone-shaped structures prevails. These suggest a striking effect of the laser wavelength on the final morphology of the metalized sample surface. However, the origin of such a difference is

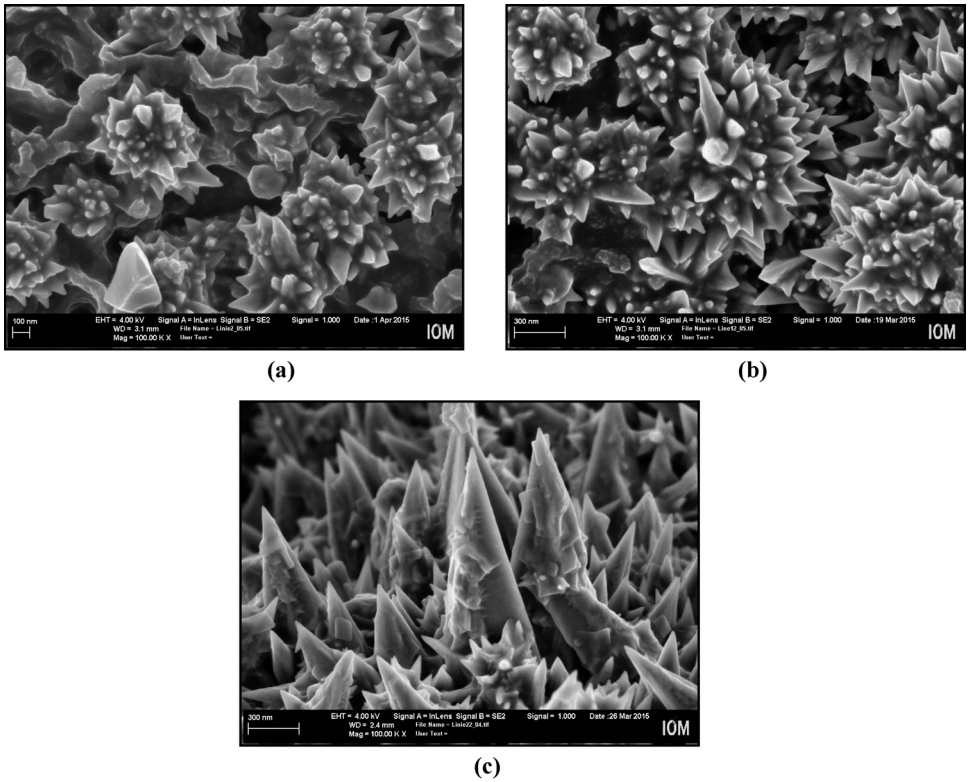

Fig. 4. Examples of SEM picture of the electro-less Ni metalized samples registered at the bottom of the trench. (a) UV laser pulses at a fluence of 1.5 J/cm^2. (b) VIS laser pulses at a fluence of 0.7 J/cm^2. (c) NIR laser pulses at a fluence of 2.7 J/cm^2. In all cases, the images refer to 83 overlapping pulses (scanning speed of 38 μm/s).

Table 2
List of the sets of fs-laser processed PDMS samples and corresponding processing conditions and results of the electro-less metallization with Ni.

No.	λ (nm)	Pulse duration	N of pulses	Energy per pulse (μJ)	Fluence (J/cm^2)	Metallization
1	263	300 fs	33	172 ± 5	2.2	Ni in form of "teeth" and "flowers"
2				138 ± 5	1.76	Not continuous with Ni "flowers"
3				82 ± 4	1.04	No Ni
4				59 ± 3	0.75	No Ni
5				59 ± 3	0.75	Uniform. Large and small Ni "teeth"
6			83	79 ± 4	1.0	Uniform. Large and small Ni "teeth"
7				125 ± 6	1.5	Uniform. Less dispersion in the size of Ni "teeth"
8	527	300 fs	33	251 ± 11	3.2	No Ni
9				150 ± 5	1.9	No Ni
10				100 ± 4	1.3	No Ni
11				56 ± 3	0.7	No Ni
12				56 ± 3	0.7	Not continuous with large Ni "flowers"
13			83	101 ± 4	1.3	Almost continuous and uniform with Ni "flowers" and large Ni "teeth"
14				142 ± 5	1.8	Almost continuous with large Ni "teeth" and some Ni flowers
15	1055	900 fs	33	307 ± 9	3.9	Uniform with large Ni "teeth"
16				204 ± 6	2.6	Almost uniform with large and small Ni "teeth"
17				119 ± 4	1.5	Almost uniform with large and small Ni "teeth" and "some flowers"
18				64 ± 3	0.8	Almost uniform with grains with Ni "teeth" with different shape
19				64 ± 3	0.8	No Ni
20			83	125 ± 9	1.6	Partially covered with Ni "teeth" in places
21				209 ± 13	2.7	Partially covered with Ni "teeth" in places
22				315 ± 5	4.0	Partially covered with Ni "teeth" in places

not yet clear at this stage and will deserve further experimental investigations in the near future. The diverse surface morphologies observed for the different samples are summarized in Table 2.

4. Conclusions

In summary, we have investigated laser surface processing of medical grade PDMS with UV, VIS and NIR fs pulses. The effects of various processing parameters, e.g. laser pulse fluence and number of overlapping pulses, on the morphology and composition of the laser produced trenches are addressed through comparison with the native materials characteristics. Our experimental findings show the formation of a c-Si Raman peak in the case of irradiation with VIS and NIR fs pulses, but not for UV fs pulses. The intensity of the c-Si peak increases with laser fluence and number of overlapping pulses. Moreover, for the higher fluence and number of overlapping pulses, the μ-Raman spectra of the processed samples present signal features assigned to broad D and G bands of amorphous carbon. The larger carbonization effects appear in case of laser treatment with NIR light. Finally, the trenches produced by higher number of overlapping pulses (i.e. 83 pulses) are successfully metalized with Ni via electro-less plating, for all three wavelengths applied. The morphology of the metalized samples presents a peculiar structure in the form of an assembly of complex nanostructures with the Ni crystallites showing "teeth" or "flower" like shapes, which deserve further analyses. Our experimental findings confirm promising expectations for the use of laser-based method exploiting femtosecond pulses for hi-tech PDMS devices micro- or nano-fabrication

Acknowledgements

The authors would like to acknowledge the support of the following bilateral joint projects between Bulgarian Academyof Sciences (BAS) and CNR (Italy) – project "Femtosecond and nanosecond laser ablation-assisted fabrication of metal and metal-oxides nanostructures" and DAAD-Germany – project 01/1 "Ion beam and laser techniques for surface nanostructuring of different materials and application to high resolution analyses (SERS)". Financial support of the BNSF under the project T02/24 entitled "New advanced method for processing nano-composite materials for creation of microsystems for medical and high-tech applications" is highly acknowledged.

References

[1] J.M. Curtis, A. Colas, Dow Corning(R) silicone biomaterials: history, chemistry & medical applications of silicones, in: B.D. Ratner (Ed.), Biomaterials Science, 2nd edition, Elsevier, London, UK, 2004, 80 pp.
[2] C. Hassler, T. Boretius, T. Stieglitz1, Polymers for neural implants, J. Polym. Sci. B: Polym. Phys. 49 (1) (2011) 18–33.
[3] L. Guo, G.S. Guvanasen, X. Liu, C. Tuthill, T.R. Nichols, S.P. DeWeerth, A PDMS-based integrated stretchable microelectrode array (is MEA) for neural and muscular surface interfacing, IEEE Trans. Biomed. Circuits Syst. 7 (1) (2013) 1–10.
[4] M. HajjHassan, V. Chodavarapu, S. Musallam, Review: neuro MEMS: neural probe microtechnologies, Sensors 8 (10) (2008) 6704–6726.
[5] S. Lacour, S. Benmerah, E. Tarte, J. Fitz Gerald, J. Serra, S. McMahon, J. Fawcett, O. Graudejus, Z. Yu, B. Morrison, Flexible and stretchable micro-electrodes for in vitro and in vivo neural interfaces, Med. Biol. Eng. Comp. 48 (10) (2010) 945–954.
[6] Editorial Overview, Lasers in surface science, Curr. Opin. Solid State Mater. Sci. (2009) 1–3, http://dx.doi.org/10.1016/j.cossms.2009.06.003.
[7] L. Laude, A. Rowley, M. Humayun, J. Weiland, Nanoscale surface activation of silicone via laser processing, US Patent, US 2008/10305320 A1 (2008).
[8] J.C. McDonald, D.C. Duffy, J.R. Anderson, D.T. Chiu, H. Wu, O.J. Schueller, G.M. Whitesides, Fabrication of microfluidic systems in poly(dimethylsiloxane), Electrophoresis 21 (1) (2000) 27–40.
[9] H. Makamba, J.H. Kim, K. Lim, N. Park, J.H. Hahn, Surface modification of poly(dimethylsiloxane) microchannels, Electrophoresis 24 (21) (2003) 3607–3619.
[10] Silicon Compounds: Silanes and Silicones, Gelest, Inc., Morrisville, PA, 2004, 560 pp.
[11] G.T. Hermanson, A.K. Mallia, P.K. Smith, Immobilized Affinity Ligand Techniques, Academic Press, San Diego, CA, 1992, pp. 454.
[12] M. Okoshi, J. Li, P.R. Herman, 157-nm F_2-laser writing of silica optical waveguides in silicone rubber, Opt. Lett. 30 (20) (2005) 2730–2732.
[13] C. Dicara, T. Robert, K. Kolev, C. Dupas-Bruzek, L.D. Laude, Excimer laser processing of silicone rubber: from understanding the process to applications, Proc. SPIE 5147 (2003) 255–265.
[14] L.D. Laude, Process for metallization of plastic materials and products there to obtained, US Patent No: 5599592 (1997).
[15] C. Dupas-Bruzek, O. Robbe, A. Addad, S. Turrell, D. Derozier, Transformation of medical grade silicone rubber under Nd:YAG and excimer laser irradiation: first step towards a new miniaturized nerve electrode fabrication process, Appl. Surf. Sci. 255 (2009) 8715–8721.
[16] P.A. Atanasov, N.N. Nedyalkov, E.I. Valova, Zh.S. Georgieva, S.A. Armyanov, K.N. Kolev, S. Amoruso, X. Wang, R. Bruzzese, M. Sawczak, G. Śliwiński, Fs-laser processing of polydimethylsiloxane and metallization, J. Appl. Phys. 116 (2) (2014) 023104.

[17] N.E. Stankova, P.A. Atanasov, N.N. Nedyalkov, T.R. Stoyanchov, K.N. Kolev, E.I. Valova, J.S. Georgieva, St.A. Armyanov, S. Amoruso, X. Wang, R. Bruzzese, K. Grochowska, G. Śliwiński, K. Baert, A. Hubin, M.P. Delplancke, J. Dille, Fs- and ns-laser processing of polydimethylsiloxane (PDMS) elastomer: comparative study, Appl. Surf. Sci. 336 (2015) 321–328.
[18] V.-M. Graubner, R. Jordan, O. Nuyken, T. Lippert, M. Hauer, B. Schnyder, A. Wokaun, Incubation and ablation behavior of poly (dimethylsiloxane) for 266 nm irradiation, Appl. Surf. Sci. 197–198 (2002) 786–790.
[19] C. Palma, M.C. Rossi, C. Sapia, E. Bemporad, Laser-induced crystallization of amorphous silicon–carbon alloys studied by Raman microscopy, Appl. Surf. Sci. 138–139 (1999) 24–28.
[20] A.C. Ferrari, Raman spectroscopy of graphene and graphite: disorder, electron–phonon coupling, doping and nonadiabatic effects, Solid State Commun. 143 (2007) 47–57.
[21] A.C. Ferrari, J. Robertson, Origin of the 1150 cm^{-1} Raman mode in nanocrystalline diamond, Phys. Rev. B 63 (2001) 121405R.